

DiffusionVMR: Diffusion Model for Video Moment Retrieval

Henghao Zhao

henghaozhao@njust.edu.cn

Nanjing University of Science and Technology
Nanjing, Jiangsu, China

Rui Yan

ruiyan@njust.edu.cn

Nanjing University of Science and Technology
Nanjing, Jiangsu, China

ABSTRACT

Video moment retrieval is a fundamental visual-language task that aims to retrieve target moments from an untrimmed video based on a language query. Existing methods typically generate numerous proposals manually or via generative networks in advance as the support set for retrieval, which is not only inflexible but also time-consuming. Inspired by the success of diffusion models on object detection, this work aims at reformulating video moment retrieval as a denoising generation process to get rid of the inflexible and time-consuming proposal generation. To this end, we propose a novel proposal-free framework, namely DiffusionVMR, which directly samples random spans from noise as candidates and introduces denoising learning to ground target moments. During training, Gaussian noise is added to the real moments, and the model is trained to learn how to reverse this process. In inference, a set of time spans is progressively refined from the initial noise to the final output. Notably, the training and inference of DiffusionVMR are decoupled, and an arbitrary number of random spans can be used in inference without being consistent with the training phase. Extensive experiments conducted on three widely-used benchmarks (i.e., QVHighlight, Charades-STA, and TACoS) demonstrate the effectiveness of the proposed DiffusionVMR by comparing it with state-of-the-art methods.

CCS CONCEPTS

- Computer systems organization → Embedded systems; Redundancy; Robotics;
- Networks → Network reliability.

KEYWORDS

Video moment retrieval, Diffusion model, Multi-modal, Denoising learning

*Corresponding author

Permission to make digital or hard copies of all or part of this work for personal or classroom use is granted without fee provided that copies are not made or distributed for profit or commercial advantage and that copies bear this notice and the full citation on the first page. Copyrights for components of this work owned by others than ACM must be honored. Abstracting with credit is permitted. To copy otherwise, or republish, to post on servers or to redistribute to lists, requires prior specific permission and/or a fee. Request permissions from permissions@acm.org.

ACM MM, October 29 - November 3, 2023, Ottawa, Canada

© 2018 Association for Computing Machinery.

ACM ISBN 978-1-4503-XXXX-X/18/06...\$15.00

<https://doi.org/XXXXXX.XXXXXXX>

Kevin Qinghong Lin

kevin.qh.lin@gmail.com

Show Lab, National University of Singapore
Singapore

Zechao Li*

zechao.li@njust.edu.cn

Nanjing University of Science and Technology
Nanjing, Jiangsu, China

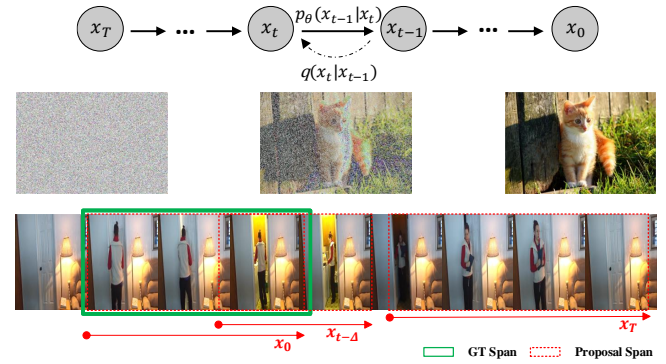


Figure 1: Diffusion model for video moment retrieval. We analogize the video moment retrieval as a denoising generation problem: a temporal span sampled from the noise is used as initialization and progressively refined to cover the target moment.

ACM Reference Format:

Henghao Zhao, Kevin Qinghong Lin, Rui Yan, and Zechao Li. 2018. DiffusionVMR: Diffusion Model for Video Moment Retrieval. In *Proceedings of Make sure to enter the correct conference title from your rights confirmation email (ACM MM)*. ACM, New York, NY, USA, 10 pages. <https://doi.org/XXXXXX.XXXXXXX>

1 INTRODUCTION

With the rapid development of the Internet, video has emerged as the most popular and content-rich medium. One important task, video moment retrieval, is to retrieve the video moments from an untrimmed video by giving natural language queries [1, 13], which has diverse applications, including media content management, intelligent monitoring, and video analysis. However, both video and natural language are temporal sequences modalities with rich semantic content. It is a challenging problem to effectively locate relevant video content specified by the language query, particularly when the content clip has various scales and unclear boundaries.

The approaches for video moment retrieval can be roughly divided into proposal-based and proposal-free paradigms. **Proposed-based methods** pre-cut various candidate clips from the whole video as the support set for retrieval via sliding windows [1, 13, 32], proposal generation networks [6, 56, 57] or multi-scale anchors [5, 51, 60, 62]. Although intuitive, these methods are time-consuming

during proposal generation and need to maintain numerous proposals throughout the algorithm process. In addition, they are sensitive to the manually designed scale of the proposals. To tackle these issues, some recent **proposal-free methods** are proposed to directly predict the start-end indices [8, 16, 35, 59] or (coordinates, saliency scores) set [24] of target moments based on a sequence of video clips, which are more efficient and flexible for practical applications. However, they are usually inferior in performance to contemporaneous proposal-based methods. Besides, these methods rely on fixed-number queries and cannot scale the moment number flexibly in the inference phase.

Inspired by the recent successful application of diffusion models to object detection [20, 47, 49], we aim to reformulate the video moment retrieval task as a denoising generation problem in this work. Diffusion models are essentially the stochastic diffusion process that adds noise to the sample and trains a model to remove the noise to learn the original data distribution. Based on this, we might be able to analogize the video moment retrieval to a noise-to-image generation task, as shown in Figure 1. A set of temporal spans sampled from the noise can be used as initialization. Besides, the location and width of spans can be gradually optimized until they can cover the target moment span perfectly. As the first work in this field to explore the denoising generation problem, it is challenging to uncover the relationship among the text query, video content, noisy span, and target moment.

To this end, we propose a novel denoising generation framework, namely DiffusionVMR, which executes the conditional denoising generation of the temporal span for video moment retrieval. DiffusionVMR contains a cross-modal encoder and a denoising decoder. **Cross-modal Encoder** is implemented by several self-attention blocks, designed to perform video-text cross-modal interaction, and then the output video representation will be used to decode the span. **Denoising Decoder** is a crucial component of our denoising process, which contains multiple cascading denoising layers. Specifically, each layer first samples the video representation corresponding to the current noisy span as the initial feature, followed by a feature-based denoising process. The location and width of the span are finally updated by the denoised features. During training, Gaussian noise is added to corrupt the ground truth temporal span, and the model is trained by learning how to reverse this process by the denoising decoder. In the inference phase, the learned reversed diffusion process progressively adjusts the initial noise to the conditional distribution. Notably, DiffusionVMR can sample multiple times during inference. Therefore, the progressive refinement process exists not only between different denoising layers in a single decoder but also between decoders that are executed multiple times. DiffusionVMR inherits the advantages of the denoising generation framework.

In contrast to proposal-based methods, DiffusionVMR does not need to maintain a large number of proposals as candidates. Instead, it directly samples proposals from the noise as initialization. Compared to the Moment-DETR [24], the training and inference of DiffusionVMR are decoupled. An arbitrary number of random spans can be used in inference without being consistent with the training phase. Extensive experiments conducted on three video moment retrieval benchmarks demonstrate the effectiveness of the

DiffusionVMR, especially achieving 9.19% improvements in average mAP in the QVHighlights dataset compared to the baseline [24].

The main contributions of this work are summarized in three folds:

- A novel framework for video moment retrieval is proposed in this paper, which reformulates the task as a conditional denoising generation process. Especially, we introduce a new approach under this framework, named DiffusionVMR, specifically designed to execute the conditional denoising generation of the temporal span.
- As a proposal-free approach, the inference candidate of DiffusionVMR is directly sampled from noise and progressively refined to the final output. Besides, the training and inference of the DiffusionVMR are decoupled, making the approach more flexible.
- Extensive experiments conducted on three challenging datasets, i.e. QVHighlight [24], Charades-STA [13] and TACoS [42], demonstrate the effectiveness of the proposed method.

2 RELATED WORK

This section will review the progress of video moment retrieval and diffusion models.

2.1 Video Moment Retrieval

The approaches in this task can be divided into two paradigms: proposal-based and proposal-free. The proposal-based paradigm performs various proposal generation techniques and essentially depends on ranking proposal candidates. The early methods usually pre-cut various candidates through sliding windows strategy [1, 13, 32] or proposal generation networks [6, 56, 57]. Inspired by some works [27, 41] in object detection, several methods [5, 58, 60] have been proposed to generate proposals by defining multi-scale anchors. These methods typically generate proposals on top of the video representation and maintain them sequentially or hierarchically. In addition, 2D map as a special proposal construction method has also attracted much attention. A representative work is proposed by Zhang et al. [62]. It collects clip features within a specific time to obtain moment representations and constructs a 2D temporal adjacent network to enumerate all moments in a video as proposals. The proposal-free paradigm, in contrast, directly predicts the start and end boundaries of target moments. Most of the proposal-free method [8, 16, 35, 59] utilizes the query-video representation to regress the target boundaries. Some other methods [19, 52, 55] adopt reinforcement learning, which simulates the decision-making process of humans but is difficult to optimize. Besides, Moment-DETR [24] is a special proposal-free method that views the task as a direct set prediction problem. In this method, paired video and text features are input into the encoder for interaction, resulting in features called Memory. The purpose of the model is to learn a set of moment queries with varying temporal scales in the decoder, which are used to determine whether exist the corresponding scale features in the Memory as a result. However, the method still relies on a set of learnable queries with relatively fixed positional semantics learned during training. Our proposed framework follows the proposal-free paradigm but reformulates

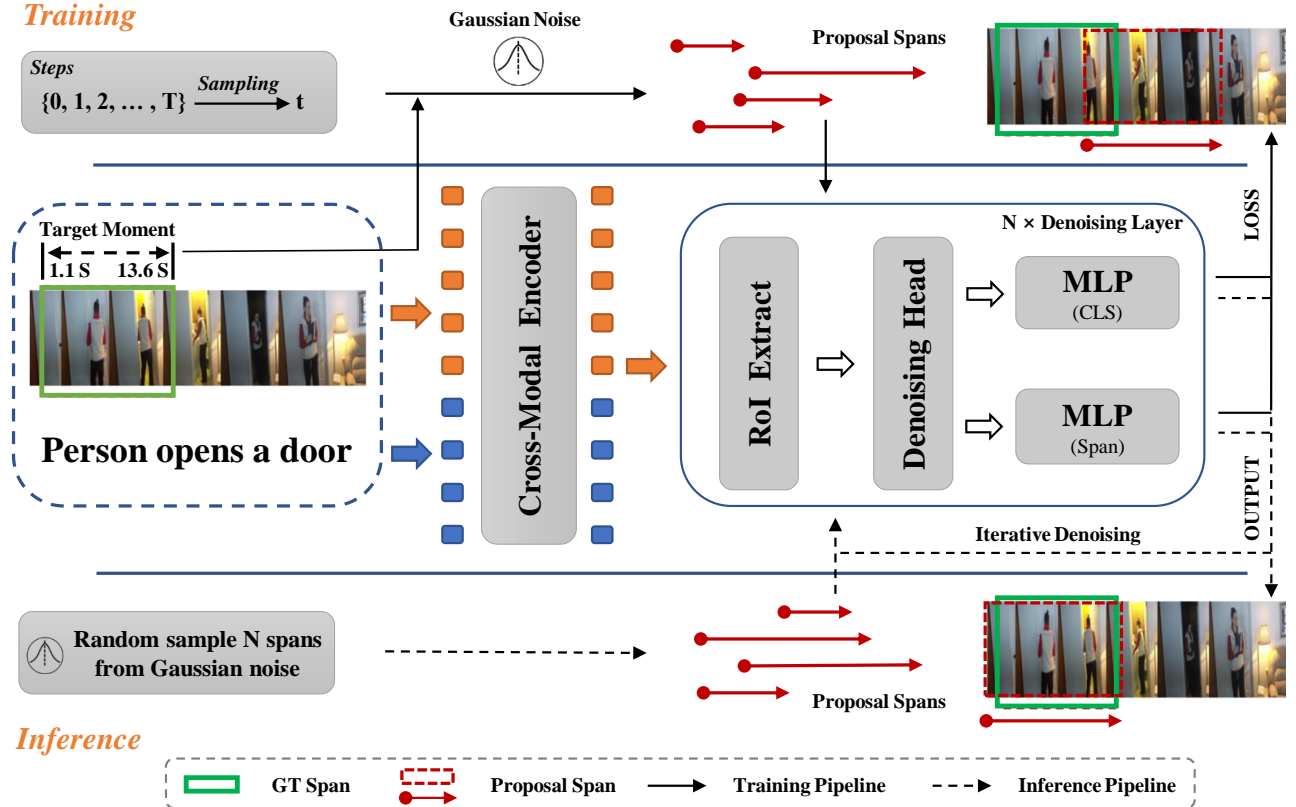


Figure 2: Overview of the proposed DiffusionVMR for video moment retrieval task. DiffusionVMR comprises a cross-modal encoder and a denoising decoder. The cross-modal encoder is used to construct the denoising generation condition, i.e. query-based video representation. The denoising decoder is composed of N cascading denoising layers that restore the noise proposal span to the target. In the training phase, the target moment undergoes t -step random diffusion processes and then is provided to the denoising decoder as the noise proposal span. Each layer in the denoising decoder takes video representation and noise proposal span as input and outputs the new span updated by the denoised representation. In inference, the noise proposal spans are directly sampled from Gaussian noise, and the final output from the decoder is used as the result.

the task as a conditional denoising generation process, which is different from the above approach.

2.2 Diffusion Models

The diffusion model [20, 47, 49] is a type of neural network that utilizes a stochastic diffusion process, inspired by thermodynamics. The process of it involves adding noise to the sample and training a model to reverse this process to learn the original data distribution. It has shown promising results in various generative tasks, such as image generation [11, 37, 44], audio generation [21, 38], and natural language generation [2, 26]. Most recently, the diffusion model technique has been applied to some discriminative visual understanding tasks, such as segmentation [3, 53], detection [9], and visual grounding [10], owing to its powerful modeling capacity. However, there have been no research or discussions for the diffusion model applied in the video moment retrieval task. In this work, we incorporate denoising learning into the video moment retrieval task by drawing on the diffusion strategy and exploring a new proposal-free framework. This framework avoids human

priors or hand-crafted components, samples candidates directly from noise, and progressively refines them from the initial noise to the final output.

3 APPROACH

The diffusion model [20, 47, 49] has recently redefined the framework for various discriminative tasks [3, 9, 10] in computer vision. Due to its iterative refinement properties, the diffusion model can progressively uncover the relationship between text queries, video content, and their corresponding timestamps. This makes the diffusion model ideal for proposal-free video moment retrieval tasks. Given a video-text pair, the input video $V = [v_0, v_1, \dots, v_{N_v}]$ is consistent with N_v clips and the input text query $Q = [q_0, q_1, \dots, q_{N_q}]$ is consistent with N_q tokens. The primary objective of the task is to identify one or multiple pairs of timestamps, denoted by τ_s and τ_e , $0 \leq \tau_s \leq \tau_e \leq N_v$. The model should ensure that the video clips within the paired timestamps have the same semantic content as the text query. The moment, which is defined by paired timestamps, can also be represented as a temporal span $s = (s_c, s_w)$,

where $s_c = (\tau_e + \tau_s)/2$, $s_w = (\tau_e - \tau_s)$. This section first provides an overview of the diffusion model, followed by the pipeline of the proposed model. The cross-modal encoder is introduced in Section 3.3 and the denoising decoder is introduced in Section 3.4. Finally, the loss function utilized in this model is presented in Section 3.5.

3.1 Preliminary

In this section, we provide a brief overview of the diffusion model. The forward process of the diffusion model is based on a stochastic diffusion process, where a sequence of Gaussian noise is iteratively added to the true data distribution, gradually reducing the quality of the ground truth. This process can be represented as follows:

$$\mathbf{x}_t := \sqrt{\alpha_t} \mathbf{x}_{t-1} + \sqrt{1 - \alpha_t} \epsilon, \quad (1)$$

where \mathbf{x}_t is the noisy sample at the diffusion step t . ϵ is the Gaussian noise. $\alpha_t = 1 - \beta_t$ is a trade-off parameter that determines the rate of the noise added to the sample. β_t is a pre-defined noise variance schedule. Following this step, the data distribution at the next diffusion step can be obtained by adding noise to the previous distribution, forming a Markov chain. As the number of diffusion steps increases, the distribution gradually deteriorates until it approaches a Gaussian noise. Actually, we can directly obtain \mathbf{x}_t from \mathbf{x}_0 without recursion [47],

$$\begin{aligned} q(\mathbf{x}_t | \mathbf{x}_0) &:= \mathcal{N}(\mathbf{x}_t; \sqrt{\bar{\alpha}_t} \mathbf{x}_0, (1 - \bar{\alpha}_t) \mathbf{I}) \\ &:= \sqrt{\bar{\alpha}_t} \mathbf{x}_0 + \sqrt{1 - \bar{\alpha}_t} \epsilon, \end{aligned} \quad (2)$$

where $\bar{\alpha}_t := \prod_{i=0}^t \alpha_i$. $\epsilon \sim \mathcal{N}(\mathbf{0}, \mathbf{I})$ is sampled from a normal distribution.

The reverse process or denoising process involves mapping the noisy sample $\mathbf{x}_t \sim \mathcal{N}(\mathbf{0}, \mathbf{I})$ back to the original sample \mathbf{x}_0 progressively. One step in the denoising process can be defined as:

$$p_\theta(\mathbf{x}_{t-1} | \mathbf{x}_t) := \mathcal{N}(\mathbf{x}_{t-1}; \mu_\theta(\mathbf{x}_t, t), \Sigma_\theta(\mathbf{x}_t, t)). \quad (3)$$

Assuming that we can estimate \mathbf{x}_0 from \mathbf{x}_t through the neural network $f_\theta(\mathbf{x}_t, t)$, based on Bayes' theorem [47],

$$q(\mathbf{x}_{t-1} | \mathbf{x}_t, \mathbf{x}_0) := \mathcal{N}(\mathbf{x}_{t-1}; \tilde{\mu}(\mathbf{x}_t, \mathbf{x}_0), \tilde{\beta}_t \mathbf{I}). \quad (4)$$

To optimize the neural network $f_\theta(\mathbf{x}_t, t)$, a mean squared error loss can be used as:

$$L_{\text{train}} = \frac{1}{2} \|f_\theta(\mathbf{x}_t, t) - \mathbf{x}_0\|^2. \quad (5)$$

3.2 Model Overview

The purpose of DiffusionVMR is to learn the conditional distribution of the target moments via denoising learning. As shown in Figure 2, the proposed model consists of a cross-modal encoder and a denoising decoder. The cross-modal encoder is used to construct the denoising generation condition, i.e. query-based video representation. The denoising decoder is composed of multiple cascading denoising layers that restore the noise proposal span to the target. It takes video representations and noise proposal spans as input and outputs the new spans updated by the denoised representations as a result.

Training pipeline. DiffusionVMR implements a diffusion process $[X_0, X_1, \dots, X_T]$ from the ground truth X_0 to noise span X_T . When

the number of diffusion steps T is large enough, X_T approaches pure noise. The model is trained to learn the underlying distribution of moment localization from the denoising process \hat{X}_T to \hat{X}_0 .

Before denoising learning, four preparatory works need to be done. Firstly, since the number of temporal spans varies across videos, the random temporal span is added to pad the ground truth to a fixed number N . The padded ground truth $X_0 \in \mathbb{R}^{N \times 2}$ is normalized. Secondly, a random diffusion step T is defined for each sample to specify the number of forward diffusion steps. Thirdly, Gaussian noises are added to the padded ground truth X_0 based on Eq.2 and diffusion step T . The noise is controlled by a predefined accumulative noise schedule. Lastly, the cross-modal encoder h_ψ is used to obtain the text query-guide video representation \mathbf{M}_V according to Eq.7.

Once the corrupted proposal temporal spans are created, the decoder g_φ is used to denoise,

$$\hat{\mathbf{p}}_s, \hat{\mathbf{p}}_c = g_\varphi(X_T, T, \mathbf{M}_V), \quad (6)$$

where the output $\hat{\mathbf{p}}_s \in \mathbb{R}^{N \times 2}$ from denoising decoder indicates the predicted spans. $\hat{\mathbf{p}}_c \in \mathbb{R}^{N \times 2}$ is the predicted class labels. Following [24], we assign it a foreground label if it matches with the ground truth and the background label otherwise. The decoder takes three inputs: X_T and \mathbf{M}_V are used in Eq.8 to obtain the proposal features f_p corresponding to corrupted proposal spans. The diffusion step T allows the model to denoise at different noise intensities. Since the prediction and the ground truth are not one-to-one matchings, bipartite matching is used to assist in calculating the loss. Notably, due to the instability of bipartite matching in the early stage of training, gradually increasing the number of proposals is recommended to improve convergence speed.

3.3 Cross-modal Encoder

The purpose of the cross-modal encoder is to model the sequence context and facilitate cross-modal interaction. Following [24], we first utilize off-the-shelf fixed visual and text backbone to extract the representation of the video and text query. Then, the features of video and text are concatenated and fed into the cross-modal encoder. The output from the cross-modal encoder is called Memory, following the convention.

More specifically, for N_v video clips, a sequence of video clips embedding $\mathbf{E}_V = [\mathbf{e}_0, \mathbf{e}_1, \dots, \mathbf{e}_{N_v}]$ is obtained from a fixed visual backbone. Similarly, a sequence of word token embedding $\mathbf{E}_Q \in \mathbb{R}^{N_q \times D_q}$ can be obtained from a fixed text backbone for use as text query input. In order to feed video sequence embedding and text sequence embedding into the encoder for interaction, the MLP is used to project the video and text features into the common space with dimension D . The encoder h_ψ is a stack of six layer Transformers with the multi-head self-attention and a feed-forward network as,

$$[\mathbf{M}_V, \mathbf{M}_Q] = h_\psi [\mathbf{E}_V, \mathbf{E}_Q] \quad (7)$$

where $\mathbf{M}_V \in \mathbb{R}^{N_v \times D}$ and $\mathbf{M}_Q \in \mathbb{R}^{N_q \times D}$ are the video memory tokens and text memory tokens output from the encoder, respectively. After multi-layer Transformer interactions, we assume the decoder can generate cross-modal representations with contextual semantic contents for subsequent feature-based denoising learning.

3.4 Denoising Decoder

The purpose of the denoising decoder is to progressively restore the noisy proposal spans to the ground truth. It is composed of six cascading denoising layers. As shown in Figure 2, the denoising layer consists of a RoI feature extract module, a denoising head, and two MLP prediction heads. Specifically, each layer takes a set of noisy proposal span as input and crops the corresponding clip features from the video memory M_V . Subsequently, these features are sent to the denoising head for denoise and output the new spans updated by the denoised representations.

As an example, we consider a noisy proposal span X_T . To extract the corresponding feature from the video memory M_V , we employ RoI feature extract module as,

$$f_p = \rho[\phi(M_V, X_T)] \quad (8)$$

where ϕ is the 1-D RoI alignment and ρ is the average pooling. Then, the features f_p are sent to the denoising head. The detection head is implemented with reference to [50], which is composed of a self-attention module, a dynamic interactive module, and a feed-forward network. The final regression prediction is completed by a 3-layer MLP. The prediction result of the MLP is a 2-D vector that represents the center point and width of the temporal span, respectively. For iteration structure, the newly generated temporal spans are served as the proposal spans for the next stage to regress more precise boundaries. The classification prediction is output by an MLP. Our decoder differs fundamentally from DETR in that we do not use the learnable query updated through backpropagation, and we explicitly model the features of the proposal span through temporal RoI alignment to refine them progressively. The diffusion model allows iterative sampling in the inference process. The full decoder is reused, and the parameters are shared across different steps. The step of the inference process is specified by timestep embedding.

3.5 Objective Function

To compute the loss, the Hungarian algorithm [23] is adopted to find the optimal bipartite assignment,

$$\hat{\kappa} = \operatorname{argmin}_{\kappa} \sum_i^N \mathcal{L}_{\text{match}}(P^i, \hat{P}^{\kappa(i)}), \quad (9)$$

$\hat{P} = \{(\hat{p}_s^i, \hat{p}_c^i)\}_{i=1}^N$ is a set of predictions. P is a set of ground truths. $\mathcal{L}_{\text{match}}(\cdot)$ is the matching cost function between the ground truth and the prediction,

$$\mathcal{L}_{\text{match}}(P^i, \hat{P}^{\kappa(i)}) = -\hat{P}_c^{\kappa(i)} + \mathcal{L}_{\text{span}}(P_s^i, \hat{P}_s^{\kappa(i)}). \quad (10)$$

Based on the optimal assignment $\hat{\kappa}$, the loss can be obtain by the following function,

$$\mathcal{L} = \lambda_{\text{class}} \mathcal{L}_{\text{class}} + \lambda_{\text{span}} \mathcal{L}_{\text{span}} + \lambda_{\text{saliency}} \mathcal{L}_{\text{saliency}}, \quad (11)$$

where $\lambda_{\text{class}}, \lambda_{\text{saliency}} \in \mathbb{R}$ are the trade-off hyper-parameters to balancing the two terms. $\mathcal{L}_{\text{class}}$ is the cross-entropy loss used to measure whether the predicted moment is correctly classified as foreground or background. $\mathcal{L}_{\text{span}}$ is used to measure the discrepancy between the moment of the ground truth and the prediction, formally,

$$\mathcal{L}_{\text{span}} = \lambda_{L1} \mathcal{L}_{L1}(P_s^i, \hat{P}_s^{\hat{\kappa}(i)}) + \lambda_{\text{iou}} \mathcal{L}_{\text{iou}}(P_s^i, \hat{P}_s^{\hat{\kappa}(i)}), \quad (12)$$

where the \mathcal{L}_{iou} is 1-D IoU loss. The denoising process in Diffusion-VMR relies on the query-guide video representation, which makes the quality of features obtained by the cross-modal encoder crucial for learning. The saliency loss $\mathcal{L}_{\text{saliency}}$ is introduced to optimize the quality of features generated by the encoder,

$$\mathcal{L}_{\text{saliency}} = \mathcal{L}_{\text{hinge}} + \mathcal{L}_{\text{contra}}. \quad (13)$$

The saliency loss is composed of a hinge loss $\mathcal{L}_{\text{hinge}}$ and a contrastive loss $\mathcal{L}_{\text{contra}}$. $L_{\text{hinge}} = \max(0, \Delta + S^{\text{low}} - S^{\text{high}})$ is used to optimize the saliency score within given video-text pairs. $\Delta \in \mathbb{R}$ is the margin. On the other hand, the contrastive loss $\mathcal{L}_{\text{contra}}$ constructs negative pairs from irrelevant video and text, making query-relevance video clips in positive pairs yield a higher saliency score than the negative pair video clips.

Inference. Once the training is completed, the DiffusionVMR can reconstruct the distribution of moment localization from arbitrary noise levels. Therefore, proposal spans are sampled from pure noise as \hat{X}_T and used to perform the denoising process $[\hat{X}_T, \hat{X}_{T-1}, \dots, \hat{X}_0]$. We assume that \hat{X}_0 can approximate the underlying ground-truth distribution and regard it as the final result. Skipping some sampling steps can speed up the denoising process [47], allowing for variable numbers of sampling steps during inference. In addition, the number of initial proposal spans during inference does not need to be the same as in training.

4 EXPERIMENTS

In this section, the effectiveness of the proposed method is validated for the video moment retrieval task. The datasets, implementation details, and evaluation metrics are introduced in Section 4.1. Subsequently, the proposed method is compared with the state-of-the-art approaches in Section 4.2. Finally, ablation studies and qualitative results on the QVHighlight dataset are shown in Section 4.3 and Section 4.4.

4.1 Experiment Setting

Datasets. Experiments are conducted on the following three publicly used datasets.

- **QVhighlight** [24] is a recent benchmark designed for video moment retrieval and highlight detection from videos given natural language. It consists of 10,310 samples annotated with human-written text queries and 10,148 videos. Each query is associated with multiple moments in a video. Experiments are conducted on the standard split, i.e., 7,218 query-moment pairs for training, 1,550 for validation, and 1,512 for testing. Notably, QVHighlights provides a fair evaluation since the evaluation of the test split results requires submission to the server.
- **Charades-STA** [13] is a dataset created by adding sentence temporal annotations on Charades [45]. It consists of 6,672 videos and provides 16,124 query-moment pairs for the video moment retrieval task. The average video and moment lengths are 30.60 seconds and 8.09 seconds, respectively. Similar to the previous work [24, 34], we use 12,404 query-moment pairs for training and 3,720 pairs for testing.

Table 1: Comparisons on the test split of QVHighlights dataset for video moment retrieval. \dagger indicates the method are not suitable for direct comparison due to the extra usage of audio features. The best results are in bold and the second-best ones are underlined.

Method	R@1			mAP	
	@0.5	@0.7	@0.5	@0.75	@Avg.
MCN [1]	11.41	2.72	24.94	8.22	10.67
CAL [12]	25.49	11.54	23.40	7.65	9.89
CLIP [40]	16.88	5.19	18.11	7.00	7.67
XML [25]	41.83	30.35	44.63	31.73	32.14
XML+ [24]	46.69	33.46	47.89	34.67	34.90
Moment-DETR [24]	52.89	33.02	54.82	29.40	30.73
UMT \dagger [34]	<u>56.23</u>	<u>41.18</u>	53.83	<u>37.01</u>	36.12
DiffusionVMR (ours)	61.61	44.49	61.55	40.17	39.92

- **TACoS** [42] is selected from the MPII Cooking Composite Activities dataset [43], which was originally developed for human activity recognition under specific scenes. It contains 127 videos and 18,818 moment-query pairs, with an average of 148.17 annotations per video. Experiments are conducted on the standard split, i.e., 10,146 query-moment pairs for training, 4,589 for validation, and 4,083 for testing.

Implementation details. PyTorch is adopted as the experimental environment. The input video frames are limited to 75 per video and the number of words is limited to 32 for a query. The beyond tokens will be truncated. The hidden dimension of the model is set to $D = 512$. The maximum diffusion step is set to $T = 1000$. All experiments are conducted on 1×NVIDIA RTX 3090 GPU. The hyperparameter used in loss function are set to $\lambda_{L1} = 10$, $\lambda_{iou} = 2$, $\lambda_{class} = 4$ and $\lambda_{saliency} = 1$. The encoder consists of 6 self-attention layers, and the decoder comprises 6 cascading denoising layers. In training, the proposed model is trained for 400 epoch and the checkpoint with the best validation performance is selected for testing. The optimizer is AdamW with the initial learning rate $1e^{-4}$ and the weight decay $1e^{-4}$. The weights of our model are randomly initialized using Xavier initialization [17]. We gradually increase the number of proposals from 1 to 20 during training. In inference, we determine the number of proposals using a grid search strategy, while keeping the sampling step as 1. We use the following dataset features in this experiment: officially released SlowFast and CLIP features for the QVHighlights dataset [24], SlowFast and CLIP features for the Charades-STA [24], VGG features for the Charades-STA [34], and C3D features for the TACoS [46].

Metrics. $Recall@K$ with IoU thresholds M ($RK@M$), mAP with IoU thresholds M ($mAP@M$), and the average mAP ($mAP@Avg$) are utilized as evaluation metrics, which are commonly used in video moment retrieval tasks. A higher IoU means that the two moments should match better. Following the convention, we adopt $R1@{0.1, 0.3, 0.5, 0.7}$, $mAP@{0.5, 0.75}$ in the experiments. All metrics used in the experiments are as high as better.

4.2 Comparison with State-of-the-arts

In this section, the proposed method is compared with the state-of-the-art methods on three benchmarks, respectively.

Table 2: Comparisons on the test split of Charades-STA dataset for video moment retrieval. Opti. means the optical flow. SF+C means the feature of Slowfast and CLIP are concatenated. The best results are in bold and the second-best ones are underlined.

Method	Feat.	R1@0.5	R1@0.7
SAP [7]	VGG	27.42	13.36
SM-RL [52]	VGG	24.36	11.17
TripNet [18]	VGG	36.61	14.50
MAN [60]	VGG	41.24	20.54
2D-TAN [62]	VGG	40.94	22.85
FVMR [14]	VGG	42.36	24.14
UMT [34]	VGG+Opti.	<u>49.35</u>	<u>26.16</u>
DiffusionVMR (ours)	VGG	54.65	32.26
CAL [12]	SF+C	47.31	30.19
2D-TAN [62]	SF+C	39.70	23.31
VSLNet [61]	SF+C	47.31	30.19
IVG-DCL [36]	SF+C	50.24	<u>32.88</u>
Moment-DETR [24]	SF+C	<u>53.63</u>	31.37
DiffusionVMR (ours)	SF+C	55.11	33.74

Table 3: Comparisons on the test split of TACoS dataset for video moment retrieval. The best results are in bold and the second-best ones are underlined.

Method	R1@0.1	R1@0.3	R1@0.5
MCN [1]	14.42	-	5.58
CTRL [13]	24.32	18.32	13.30
MCF [54]	25.84	18.64	12.53
TGN [5]	41.87	21.77	18.90
ACRN [31]	24.22	19.52	14.62
ROLE [33]	20.37	15.38	9.94
VAL [48]	25.74	19.76	14.74
ACL-K [15]	31.64	24.17	20.01
CMIN [28]	36.68	27.33	19.57
SM-RL [52]	26.51	20.25	15.95
SLTA [22]	23.13	17.07	11.92
SAP [7]	31.15	-	18.24
TripNet [18]	-	23.95	19.17
2D-TAN [62]	47.59	37.29	25.32
CSMGAN [29]	42.74	33.90	27.09
FIAN [39]	39.55	33.87	28.58
LGN [30]	52.46	41.71	30.57
SMRN [4]	50.44	42.49	32.07
VLG-Net [46]	<u>57.21</u>	45.46	34.19
DiffusionVMR (ours)	58.09	<u>45.41</u>	<u>32.44</u>

QVHighlights. The QVHighlights dataset provides official features and online test split evaluation, enabling the production of fair and convincing results. Table 1 shows the performance comparison on the QVHighlights tests split. DiffusionVMR achieves the most exceptional performance across all metrics with a clear margin. It demonstrates the effectiveness of the proposed approach. Our approach exhibits an improvement of over 6% relative to the baseline Moment-DETR, especially with the significant improvement on the

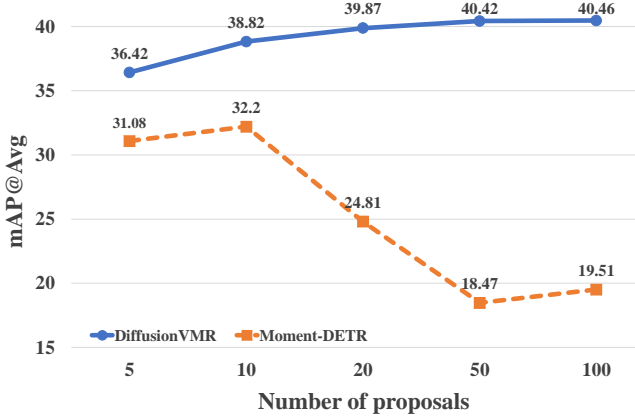


Figure 3: Effectiveness of different numbers of proposals on QVHighlights val split. The training and inference of DiffusionVMR are decoupled. As the number of proposals in inference increases, the performance of DiffusionVMR improves steadily.

more stringent metrics exceeding 10%. Moreover, the improvement of DiffusionVMR is across the board, as reflected by the significant increase in the average mAP. In contrast, Moment-DETR performs better only at lower IoU thresholds, i.e. $R1@0.5$ and $mAP@0.5$. UMT, which additionally employs audio features and aims to improve cross-modal interactions, also lags behind DiffusionVMR in performance, even when using only visual features.

Charades-STA. DiffusionVMR is compared with existing methods under different feature settings. The features used in this section are listed in the table to ensure fair comparisons. As shown in Table 2, DiffusionVMR consistently outperforms other methods across all settings. In the setting of using VGG features, DiffusionVMR can achieve significant performance gains, whether compared to proposal-based approaches (e.g., 2D-TAN) or proposal-free approaches (e.g., UMT). Even when using SlowFast+CLIP features, DiffusionVMR still outperforms the baseline Moment-DETR, providing further evidence of the effectiveness of our proposed method. **TACoS.** As demonstrated in Table 3, DiffusionVMR outperforms most of the methods, showcasing its effectiveness. VLG-Net generates numerous proposals, whereas our method achieves comparable results by using only a few candidates sampled from noise.

4.3 Ablation Studies

Number of proposals. Decoupling the training and inference of DiffusionVMR is a crucial characteristic that allows the use of an arbitrary number of randomly initialized proposals for retrieval, without the need for consistency with the training phase. To investigate how the number of proposals affects model performance in inference, we set the proposal number in the range of 5 to 100 and report the results in terms of the $mAP@Avg$ metric. As a comparison, we also report the performance variation of Moment-DETR under different moment queries. The results of Moment-DETR are taken from the original paper. Figure 3 shows that the performance of DiffusionVMR steadily improves as the number of proposals

Query: Dogs are pulling the bobsled.

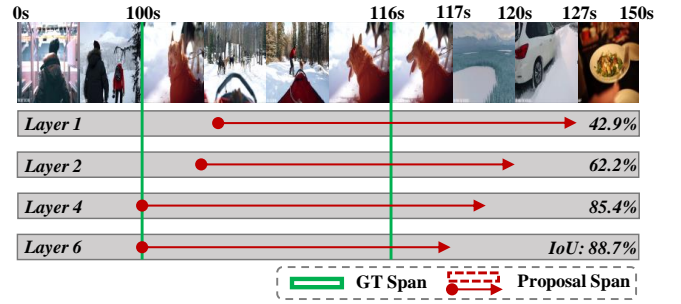


Figure 4: Effectiveness of different numbers of denoising layer on QVHighlights val split. As the layer deepens, the IoU between the prediction span and ground-truth increases.

Table 4: Effectiveness of different number of the sampling steps on QVHighlights val split.

Sampling Step	R@1		mAP	Time Cost(s)	
	R1@0.5	R1@0.7	@Avg	BS=1	BS=100
1	61.56	47.51	41.43	0.061	1.825
2	61.87	47.55	41.48	0.116	3.367
4	61.15	47.07	41.35	0.194	6.818
6	60.81	47.11	41.17	0.273	10.651
8	60.96	47.27	41.32	0.354	15.063

in inference increases. More randomly initialized proposals provide more diversity for retrieval. In contrast, Moment-DETR shows performance degradation when the number of moment queries exceeds 10. It makes sense to decouple training and inference. DiffusionVMR can be flexibly applied to tasks with different numbers of targets without re-training. Additionally, it eliminates the need to maintain a mass of proposals as the support set for retrieval.

Progressive refinement. As another characteristic of our proposed approach, it can progressively refine the time span boundaries during inference. DiffusionVMR achieves this refinement in two ways: 1) between different denoising layers of the decoder and 2) through multiple samplings during inference. The latter method iteratively refines the boundaries between different sampling steps by specifying the different timestep T . The progressive refinement between denoising layers is illustrated in Figure 4. The IoU growth as the layer increases, indicating a more accurate boundary of the proposal span. The results of multiple sampling are reported in Table 4. Unfortunately, we did not noticeably benefit from increasing the sample step. One possible explanation is that the model can eliminate the noise by multiple denoising layers in just one sampling step, causing performance to reach saturation. On the other hand, multiple sampling steps result in a significant time cost increase that is unfriendly to real applications. After careful consideration, we opted to use only one sampling step and six denoising layers in the experiments.

Effectiveness of the loss components. We investigate the composition of the loss used in our model. To evaluate the impact of each loss, we turn off one at a time and report the results in Table

Query: The Colosseum shown from many angles.



DiffusionVMR



Moment-DETR



Query: People walk through a glass tunnel.



DiffusionVMR



Moment-DETR



Figure 5: Video moment retrieval examples on QVHighlights val split. we only visualize the time spans corresponding to the top K confidence scores. The green box means the ground truth.

Table 5: Effectiveness of different components of the loss on QVHighlights val split.

\mathcal{L}_{Span}	$\mathcal{L}_{Salience}$	\mathcal{L}_{hinge}	\mathcal{L}_{contra}	\mathcal{L}_{class}	R@1		mAP
					R1@0.5	R1@0.7	
\times					60.32	44.97	39.68
\times					61.45	46.13	w38.99
		\times			61.74	46.45	40.32
		\times			58.90	43.16	38.62
		\times			43.03	27.68	30.84
					62.58	48.45	41.51

5. \mathcal{L}_{span} is primarily employed to constrain the accuracy of the predicted span. We observe a decrease in performance when either \mathcal{L}_1 or \mathcal{L}_{iou} loss is turned off, indicating their importance. $\mathcal{L}_{salience}$ is critical for constraining cross-modal interaction in the encoder. Since the denoising learning process is built on query-based video representation, it significantly affects the model's performance. Furthermore, our findings show that using uncorrelated pairs to learn discriminative features is beneficial for cross-modal interaction, as \mathcal{L}_{contra} provides more significant gain than \mathcal{L}_{hinge} . The video moment retrieval task has only start and end timestamps as positive samples, which results in a data imbalance problem compared to mass frames. Therefore, \mathcal{L}_{class} is used to distinguish the foreground ground-truth spans and background padding.

Effect of matching strategy. When the number of training proposals is much larger than the ground truth, it can cause instability of bipartite graph matching. This instability may arise due to the increasing number of proposals resulting in inconsistent optimization goals, particularly in the early training phase. Therefore, we recommend gradually increasing the number of training proposals from 1. The results in Table 6 demonstrate that this training strategy can significantly improve performance.

4.4 Visualization

In this section, we present the qualitative results of DiffusionVMR in Figure 5. The red arrows indicate the time spans predicted by our approach, and the blue ones correspond to the baseline Moment-DETR for comparison. Overall, our method can accurately retrieve the correct results, whether one or more targets are in the video. Notably, DiffusionVMR outperforms the baseline in terms of the accuracy of predicted time spans. The first example demonstrates that our model can handle abstract meanings and accurately capture The Colosseum shown from day to night. For the error prediction part, DiffusionVMR usually returns results closer to the query semantics than Moment-DETR, as shown in the second example, where our method identifies the show of the glass tunnel instead of an irrelevant scene.

5 CONCLUSION

In this work, we present a novel framework for the video moment retrieval task by formulating it as a conditional denoising generation

Table 6: Effectiveness of different training strategy on QVHighlights val split.

Training Strategy	R@1		mAP @Avg
	R1@0.5	R1@0.7	
Stable	58.39	42.19	37.23
Progress	59.81	45.29	39.82

process. Especially a novel approach, DiffusionVMR, is designed by us to execute the conditional denoising generation of the temporal span. Unlike the previous works, the inference candidates of DiffusionVMR are directly sampled from noise and progressively refined to the final output. Besides, the training and inference of the DiffusionVMR are decoupled, making the approach more flexible. Experimental results on QVHighlights, Charades-STA, and TACoS datasets demonstrate the effectiveness of the proposed approach. We hope that this work can inspire future research to explore the potential of the denoising generation process in this task.

REFERENCES

- [1] Lisa Anne Hendricks, Oliver Wang, Eli Shechtman, Josef Sivic, Trevor Darrell, and Bryan Russell. 2017. Localizing moments in video with natural language. In *IEEE/CVF International Conference on Computer Vision (ICCV)*. 5803–5812.
- [2] Jacob Austin, Daniel D Johnson, Jonathan Ho, Daniel Tarlow, and Rianne van den Berg. 2021. Structured denoising diffusion models in discrete state-spaces. In *Advances in Neural Information Processing Systems (NeurIPS)*. 17981–17993.
- [3] Dmitry Baranukh, Andrey Voynov, Ivan Rubachev, Valentin Khrulkov, and Artem Babenko. 2022. Label-Efficient Semantic Segmentation with Diffusion Models. In *International Conference on Learning Representations (ICLR)*.
- [4] Cheng Chen and Xiaodong Gu. 2020. Semantic modulation based residual network for temporal language queries grounding in video. In *International Symposium on Neural Networks (ISNN)*. 119–129.
- [5] Jingyuan Chen, Xinpeng Chen, Lin Ma, Zequan Jie, and Tat-Seng Chua. 2018. Temporally grounding natural sentence in video. In *Empirical Methods in Natural Language Processing (EMNLP)*. 162–171.
- [6] Shaoxiang Chen and Yu-Gang Jiang. 2019. Semantic proposal for activity localization in videos via sentence query. In *AAAI Conference on Artificial Intelligence (AAAI)*. 8199–8206.
- [7] Shaoxiang Chen and Yu-Gang Jiang. 2019. Semantic proposal for activity localization in videos via sentence query. In *AAAI Conference on Artificial Intelligence (AAAI)*. 8199–8206.
- [8] Shaoxiang Chen and Yu-Gang Jiang. 2020. Hierarchical visual-textual graph for temporal activity localization via language. In *European Conference on Computer Vision (ECCV)*. 601–618.
- [9] Shoufa Chen, Peize Sun, Yibing Song, and Ping Luo. 2022. Diffusiondet: Diffusion model for object detection. *arXiv preprint arXiv:2211.09788* (2022).
- [10] Zesen Cheng, Kehan Li, Peng Jin, Xiangyang Ji, Li Yuan, Chang Liu, and Jie Chen. 2023. Parallel Vertex Diffusion for Unified Visual Grounding. *arXiv preprint arXiv:2303.07216* (2023).
- [11] Prafulla Dhariwal and Alexander Nichol. 2021. Diffusion models beat gans on image synthesis. In *Advances in Neural Information Processing Systems (NeurIPS)*. 8780–8794.
- [12] Victor Escorcia, Mattia Soldan, Josef Sivic, Bernard Ghanem, and Bryan Russell. 2019. Temporal localization of moments in video collections with natural language. *arXiv preprint arXiv:1907.12763* (2019).
- [13] Jiyang Gao, Chen Sun, Zhenheng Yang, and Ram Nevatia. 2017. Tall: Temporal activity localization via language query. In *IEEE/CVF International Conference on Computer Vision (ICCV)*. 5267–5275.
- [14] Junyu Gao and Changsheng Xu. 2021. Fast video moment retrieval. In *IEEE/CVF International Conference on Computer Vision (ICCV)*. 1523–1532.
- [15] Runzhou Ge, Jiyang Gao, Kan Chen, and Ram Nevatia. 2019. Mac: Mining activity concepts for language-based temporal localization. In *IEEE Winter Conference on Applications of Computer Vision (WACV)*. 245–253.
- [16] Soham Ghosh, Anuva Agarwal, Zarana Parekh, and Alexander Hauptmann. 2019. Excl: Extractive clip localization using natural language descriptions. *arXiv preprint arXiv:1904.02755* (2019).
- [17] Xavier Glorot and Yoshua Bengio. 2010. Understanding the difficulty of training deep feedforward neural networks. In *International Conference on Artificial Intelligence and Statistics (AISTATS)*. 249–256.
- [18] Meera Hahn, Asim Kadav, James M Rehg, and Hans Peter Graf. 2019. Tripping through time: Efficient localization of activities in videos. *arXiv preprint arXiv:1904.09936* (2019).
- [19] Dongliang He, Xiang Zhao, Jizhou Huang, Fu Li, Xiao Liu, and Shilei Wen. 2019. Read, watch, and move: Reinforcement learning for temporally grounding natural language descriptions in videos. In *AAAI Conference on Artificial Intelligence (AAAI)*. 8393–8400.
- [20] Jonathan Ho, Ajay Jain, and Pieter Abbeel. 2020. Denoising diffusion probabilistic models. In *Advances in Neural Information Processing Systems (NeurIPS)*. 6840–6851.
- [21] Rongjii Huang, Zhou Zhao, Huadai Liu, Jinglin Liu, Chenye Cui, and Yi Ren. 2022. Prodif: Progressive fast diffusion model for high-quality text-to-speech. In *the 30th ACM International Conference on Multimedia (ACM MM)*. 2595–2605.
- [22] Bin Jiang, Xin Huang, Chao Yang, and Junsong Yuan. 2019. Cross-modal video moment retrieval with spatial and language-temporal attention. In *International Conference on Multimedia Retrieval (ICMR)*. 217–225.
- [23] Harold W Kuhn. 1955. The Hungarian method for the assignment problem. *Naval Research Logistics Quarterly* 2, 1-2 (1955), 83–97.
- [24] Jie Lei, Tamara L Berg, and Mohit Bansal. 2021. Detecting moments and highlights in videos via natural language queries. In *Advances in Neural Information Processing Systems (NeurIPS)*. 11846–11858.
- [25] Jie Lei, Licheng Yu, Tamara L Berg, and Mohit Bansal. 2020. Tvr: A large-scale dataset for video-subtitle moment retrieval. In *European Conference on Computer Vision (ECCV)*. 447–463.
- [26] Xiang Li, John Thickstun, Ishaan Gulrajani, Percy S Liang, and Tatsunori B Hashimoto. 2022. Diffusion-lm improves controllable text generation. In *Advances in Neural Information Processing Systems (NeurIPS)*. 4328–4343.
- [27] Tsung-Yi Lin, Priya Goyal, Ross Girshick, Kaiming He, and Piotr Dollár. 2017. Focal loss for dense object detection. In *IEEE/CVF International Conference on Computer Vision (ICCV)*. 2980–2988.
- [28] Zhijie Lin, Zhou Zhao, Zhu Zhang, Zijian Zhang, and Deng Cai. 2020. Moment retrieval via cross-modal interaction networks with query reconstruction. *IEEE Transactions on Image Processing* 29 (2020), 3750–3762.
- [29] Daizong Liu, Xiaoye Qu, Xiao-Yang Liu, Jianfeng Dong, Pan Zhou, and Zichuan Xu. 2020. Jointly cross-and self-modal graph attention network for query-based moment localization. In *the 28th ACM International Conference on Multimedia (ACM MM)*. 4070–4078.
- [30] Kun Liu, Huadong Ma, and Chuang Gan. 2020. Language Guided Networks for Cross-modal Moment Retrieval. *arXiv preprint arXiv:2006.10457* (2020).
- [31] Meng Liu, Xiang Wang, Liqiang Nie, Xiangnan He, Baoquan Chen, and Tat-Seng Chua. 2018. Attentive moment retrieval in videos. In *Conference of the Association for Computing Machinery Special Interest Group in Information Retrieval (ACM SIGIR)*. 15–24.
- [32] Meng Liu, Xiang Wang, Liqiang Nie, Qi Tian, Baoquan Chen, and Tat-Seng Chua. 2018. Cross-modal moment localization in videos. In *the 26th ACM International Conference on Multimedia (ACM MM)*. 843–851.
- [33] Meng Liu, Xiang Wang, Liqiang Nie, Qi Tian, Baoquan Chen, and Tat-Seng Chua. 2018. Cross-modal moment localization in videos. In *the 26th ACM International Conference on Multimedia (ACM MM)*. 843–851.
- [34] Ye Liu, Siyuan Li, Yang Wu, Chang-Wen Chen, Ying Shan, and Xiaohu Qie. 2022. Umt: Unified multi-modal transformers for joint video moment retrieval and highlight detection. In *IEEE/CVF Conference on Computer Vision and Pattern Recognition (CVPR)*. 3042–3051.
- [35] Jonghwan Mun, Minsu Cho, and Bohyung Han. 2020. Local-global video-text interactions for temporal grounding. In *IEEE/CVF Conference on Computer Vision and Pattern Recognition (CVPR)*. 10810–10819.
- [36] Guoshun Nan, Rui Qiao, Yao Xiao, Jun Liu, Sicong Leng, Hao Zhang, and Wei Lu. 2021. Interventional video grounding with dual contrastive learning. In *IEEE/CVF Conference on Computer Vision and Pattern Recognition (CVPR)*. 2765–2775.
- [37] Alex Nichol, Prafulla Dhariwal, Aditya Ramesh, Pranav Shyam, Pamela Mishkin, Bob McGrew, Ilya Sutskever, and Mark Chen. 2021. Glide: Towards photorealistic image generation and editing with text-guided diffusion models. *arXiv preprint arXiv:2112.10741* (2021).
- [38] Vadim Popov, Ivan Vovk, Vladimir Gogoryan, Tasnimadev Sadekova, and Mikhail Kudinov. 2021. Grad-tts: A diffusion probabilistic model for text-to-speech. In *International Conference on Machine Learning (ICML)*. 8599–8608.
- [39] Xiaoye Qu, Pengwei Tang, Zhikang Zou, Yu Cheng, Jianfeng Dong, Pan Zhou, and Zichuan Xu. 2020. Fine-grained iterative attention network for temporal language localization in videos. In *the 28th ACM International Conference on Multimedia (ACM MM)*. 4280–4288.
- [40] Alec Radford, Jong Wook Kim, Chris Hallacy, Aditya Ramesh, Gabriel Goh, Sandhini Agarwal, Girish Sastry, Amanda Askell, Pamela Mishkin, Jack Clark, et al. 2021. Learning transferable visual models from natural language supervision. In *International Conference on Machine Learning (ICML)*. 8748–8763.
- [41] Joseph Redmon, Santosh Divvala, Ross Girshick, and Ali Farhadi. 2016. You only look once: Unified, real-time object detection. In *IEEE/CVF Conference on Computer Vision and Pattern Recognition (CVPR)*. 779–788.

[42] Michaela Regneri, Marcus Rohrbach, Dominikus Wetzel, Stefan Thater, Bernt Schiele, and Manfred Pinkal. 2013. Grounding action descriptions in videos. *Transactions of the Association for Computational Linguistics* 1 (2013), 25–36.

[43] Marcus Rohrbach, Michaela Regneri, Mykhaylo Andriluka, Sikandar Amin, Manfred Pinkal, and Bernt Schiele. 2012. Script data for attribute-based recognition of composite activities. In *European Conference on Computer Vision (ECCV)*. 144–157.

[44] Robin Rombach, Andreas Blattmann, Dominik Lorenz, Patrick Esser, and Björn Ommer. 2022. High-resolution image synthesis with latent diffusion models. In *IEEE/CVF Conference on Computer Vision and Pattern Recognition (CVPR)*. 10684–10695.

[45] Gunnar A Sigurdsson, Gü̈l Varol, Xiaolong Wang, Ali Farhadi, Ivan Laptev, and Abhinav Gupta. 2016. Hollywood in homes: Crowdsourcing data collection for activity understanding. In *European Conference on Computer Vision (ECCV)*. 510–526.

[46] Mattia Soldan, Mengmeng Xu, Sisi Qu, Jesper Tegner, and Bernard Ghanem. 2021. Vlg-net: Video-language graph matching network for video grounding. In *IEEE/CVF Conference on Computer Vision and Pattern Recognition (CVPR)*. 3224–3234.

[47] Jiaming Song, Chenlin Meng, and Stefano Ermon. 2021. Denoising diffusion implicit models. In *International Conference on Learning Representations (ICLR)*.

[48] Xiaomeng Song and Yahong Han. 2018. VAL: Visual-attention action localizer. In *Pacific-Rim Conference on Multimedia (PCM)*. 340–350.

[49] Yang Song and Stefano Ermon. 2019. Generative modeling by estimating gradients of the data distribution. In *Advances in Neural Information Processing Systems (NeurIPS)*.

[50] Peize Sun, Rufeng Zhang, Yi Jiang, Tao Kong, Chenfeng Xu, Wei Zhan, Masayoshi Tomizuka, Lei Li, Zehuan Yuan, Changhu Wang, et al. 2021. Sparse r-cnn: End-to-end object detection with learnable proposals. In *IEEE/CVF Conference on Computer Vision and Pattern Recognition (CVPR)*. 14454–14463.

[51] Hao Wang, Zheng-Jun Zha, Liang Li, Dong Liu, and Jiebo Luo. 2021. Structured multi-level interaction network for video moment localization via language query. In *IEEE/CVF Conference on Computer Vision and Pattern Recognition (CVPR)*. 7026–7035.

[52] Weining Wang, Yan Huang, and Liang Wang. 2019. Language-driven temporal activity localization: A semantic matching reinforcement learning model. In *IEEE/CVF Conference on Computer Vision and Pattern Recognition (CVPR)*. 334–343.

[53] Julia Wolleb, Robin Sandkühler, Florentin Bieder, Philippe Valmaggia, and Philippe C Cattin. 2022. Diffusion models for implicit image segmentation ensembles. In *International Conference on Medical Imaging with Deep Learning (MIDL)*. 1336–1348.

[54] Aming Wu and Yahong Han. 2018. Multi-modal Circulant Fusion for Video-to-Language and Backward.. In *International Joint Conferences on Artificial Intelligence (IJCAI)*. 8.

[55] Jie Wu, Guanbin Li, Si Liu, and Liang Lin. 2020. Tree-structured policy based progressive reinforcement learning for temporally language grounding in video. In *AAAI Conference on Artificial Intelligence (AAAI)*. 12386–12393.

[56] Huijuan Xu, Kun He, Bryan A Plummer, Leonid Sigal, Stan Sclaroff, and Kate Saenko. 2019. Multilevel language and vision integration for text-to-clip retrieval. In *AAAI Conference on Artificial Intelligence (AAAI)*. 9062–9069.

[57] Huijuan Xu, Kun He, Leonid Sigal, Stan Sclaroff, and Kate Saenko. 2018. Text-to-clip video retrieval with early fusion and re-captioning. *arXiv preprint arXiv:1804.05113* 2, 6 (2018), 7.

[58] Yitian Yuan, Lin Ma, Jingwen Wang, Wei Liu, and Wenwu Zhu. 2019. Semantic conditioned dynamic modulation for temporal sentence grounding in videos. In *Advances in Neural Information Processing Systems (NeurIPS)*.

[59] Yitian Yuan, Tao Mei, and Wenwu Zhu. 2019. To find where you talk: Temporal sentence localization in video with attention based location regression. In *AAAI Conference on Artificial Intelligence (AAAI)*. 9159–9166.

[60] Da Zhang, Xiyang Dai, Xin Wang, Yuan-Fang Wang, and Larry S Davis. 2019. Man: Moment alignment network for natural language moment retrieval via iterative graph adjustment. In *IEEE/CVF Conference on Computer Vision and Pattern Recognition (CVPR)*. 1247–1257.

[61] Hao Zhang, Aixin Sun, Wei Jing, and Joey Tianyi Zhou. 2020. Span-based Localizing Network for Natural Language Video Localization. In *Annual Meeting of the Association for Computational Linguistics (ACL)*. 6543–6554.

[62] Songyang Zhang, Houwen Peng, Jianlong Fu, Yijuan Lu, and Jiebo Luo. 2021. Multi-scale 2d temporal adjacency networks for moment localization with natural language. *IEEE Transactions on Pattern Analysis and Machine Intelligence* 44, 12 (2021), 9073–9087.